Chapter 5

Prism & Grating

In this chapter the component matrices for the prism and grating are discussed. Additional details of the analysis, using the method outlined in Chapter 4, are found in Appendix C. The through-put of each component is also found.

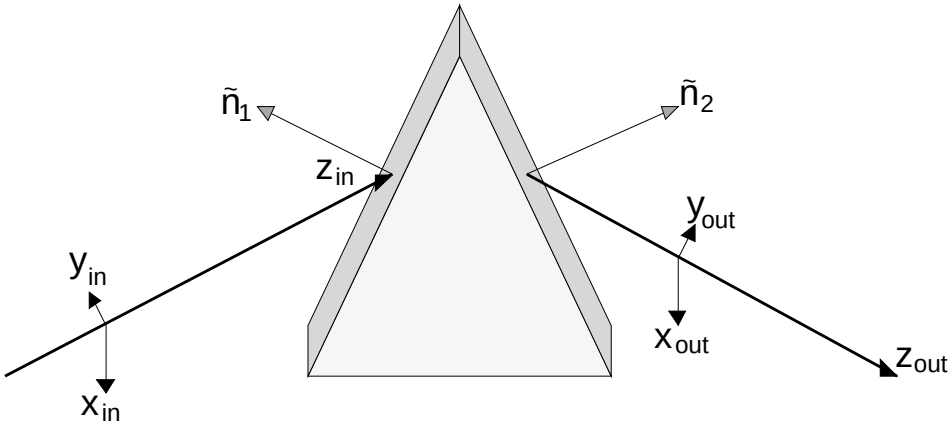

Figure 5.1: Analysis coordinates applied to the prism.

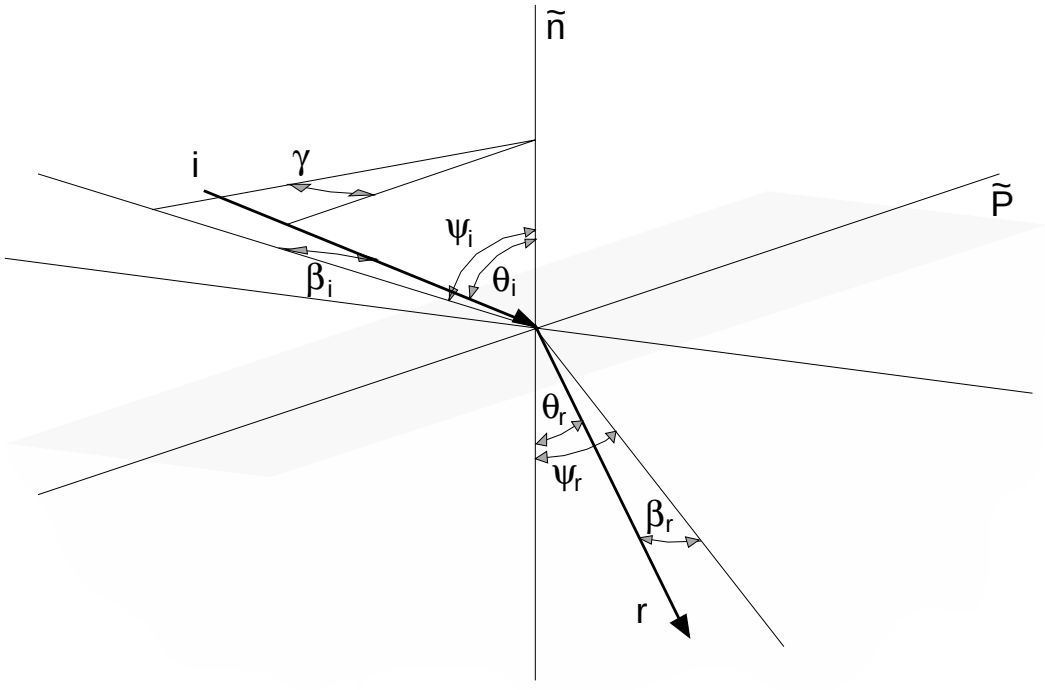

Figure 5.2: Light ray at the prism surface.

5.1 Prism Matrix P

First consider a single prism near minimum deviation, where the surface normals and all rays lie in the same plane (the principal plane). The principal (reference) ray passes through the prism at minimum deviation. Figure 5.1 shows how the chosen coordinate system, with the **Z** axis corresponding to the principal ray, relates to the prism

Because the system is symmetrical when used at (or near) minimum deviation, then the position of a ray in terms of its x, y coordinates will be maintained as it passes through the prism.

$$\begin{aligned} x_{out} &= x_{in} \\ y_{out} &= y_{in} \end{aligned} \tag{5.1}$$

Consider now what happens when the input ray, $\vec{R}_{in}$, varies by an arbitrary but small angle from the principal ray. At the surface of the prism various angles and vectors can be defined as in Figure 5.2.

The surface normal $\vec{n}$ and the vector $\vec{p}$ defines the principal plane (principal section) of the prism. The input ray i , refracted ray r , and the normal, are also co-planar. This plane, however, is rotated about the normal by an angle of γ with respect to the principal plane.

The various angles are related as follows:

$$\sin\beta = \sin\theta\sin\gamma \tag{5.2}$$

$$\sin\theta\cos\gamma = \sin\psi\cos\beta \tag{5.3}$$

$$\text{from Snell's law} \quad \sin\theta_i = n\sin\theta_r \tag{5.4}$$

$$\text{then} \quad \sin\beta_i = n\sin\beta_r \tag{5.5}$$

If i_0 is the angle of incidence of the principal ray then at the first and second surfaces respectively:

$$\begin{aligned} \psi_{i1} &= i_0 - \phi_{x.in} \\ \psi_{i2} &= i_0 + \phi_{x.out} \end{aligned} \tag{5.6}$$

and

$$\begin{aligned} \beta_{i1} &= \phi_{y.in} \\ \beta_{i2} &= \phi_{y.out} \end{aligned} \tag{5.7}$$

Because β is the angle that the ray makes with the principle plane of the prism, $\beta_{r2} = \beta_{r1}$ and from the definition of β in equation 5.7 then:

$$\phi_{y.out} = \phi_{y.in} \tag{5.8}$$

From equation 5.3

$$\sin\psi_{i1}\cos\beta_{i1} = n\sin\psi_{r1}\cos\beta_{r1} \tag{5.9}$$

Applying to the first surface:

$$\sin(i_0 - \phi_{x.in})\cos\beta_i = n\sin\left(\frac{\alpha}{2} - \Delta\psi_r\right)\cos\beta_r \tag{5.10}$$

Similarly at the second surface:

$$\sin(i_0 - \phi_{x.out})\cos\beta_i = n\sin\left(\frac{\alpha}{2} + \Delta\psi_r\right)\cos\beta_r \tag{5.11}$$

But because β is small $\beta_i \approx n\beta_r$ and $\cos\beta \approx 1$.

Adding equations 5.10 and 5.11

$$(\phi_{x.out} - \phi_{x.in})\cos i_0 \approx 0$$

giving:

$$\phi_{x.out} \approx \phi_{x.in} \tag{5.12}$$

Therefore from equations 5.1, 5.8, and 5.12 we can say that for any input ray, the corresponding output ray is described by:

$$\vec{R}_{out} = \vec{R}_{in} \tag{5.13}$$

The component matrix for the prism, P, is therefore equivalent to the unit matrix:

$$P = \begin{vmatrix} 1 & 0 & 0 & 0 \\ 0 & 1 & 0 & 0 \\ 0 & 0 & 1 & 0 \\ 0 & 0 & 0 & 1 \end{vmatrix} \tag{5.14}$$

5.2 Prism Through-put

For the uncoated, 60 degree crown glass prism a theoretical value for the through-put can be readily found. The Fresnel equations deal with polarised light (parallel or perpendicular to the surface) from an electromagnetic point of view giving the *amplitude transmission coefficients*:

$$t_\perp \equiv \left(\frac{E_{\perp t}}{E_{\perp i}}\right) \tag{5.15}$$

$$t_\parallel \equiv \left(\frac{E_{\parallel t}}{E_{\parallel i}}\right) \tag{5.16}$$

For each polarisation the ratio of incident to transmitted intensity, or *transmittance*, for each surface is given by:

$$T = \left(\frac{n_t \cos\theta_t}{n_i \cos\theta_i} \right) t^2 \tag{5.17}$$

In a prism disperser at minimum deviation we have two surfaces, 1 and 2, where for the first surface $n_{i1} = 1$ (air) and $n_{t1} = n_{glass}$. At the second surface where the beam exits the prism $n_{i2} = n_{glass}$ and $n_{t2} = 1$. Additionally $\theta_{i1} = \theta_{t2}$ and $\theta_{t1} = \theta_{i2}$. The transmittance for the complete prism is therefore:

$$\begin{aligned} T_{prism} &= T_1 \times T_2 \\ &= t_1^2 \times t_2^2 \end{aligned} \tag{5.18}$$

This, however, will only give a value for each polarisation, so an average must be taken because the light entering the prism is unpolarised.

$$T_{prism} = \frac{t_{\perp 1}^2 t_{\perp 2}^2 + t_{\parallel 1}^2 t_{\parallel 2}^2}{2} \tag{5.19}$$

As previously mentioned, the prism under consideration has a 60° apex angle and is manufactured from crown glass, $n_{glass} \approx 1.5$. The theoretical transmission can be calculated to give:

$$T_{prism} = 0.89 \tag{5.20}$$

This value, however, proves to be somewhat optimistic. Absorption of the light through approximately 5cm of glass causes a loss of about 2%. Surface scratches and contamination can (and do in this case) cause losses through scattering of the light. Measurement of the prism through-put using a laser diode and a photovoltaic cell (see Appendix B for details) yielded a value of only 80% for transmission at 670nm wavelength. A quite noticeable amount of scattering of the beam was evident at the surfaces of the prism, mainly due to fine scratches. A transmission factor of 85% will be assumed allowing for a better prism system to be implemented in the future.

$$\tau_{prism} = 0.85 \tag{5.21}$$

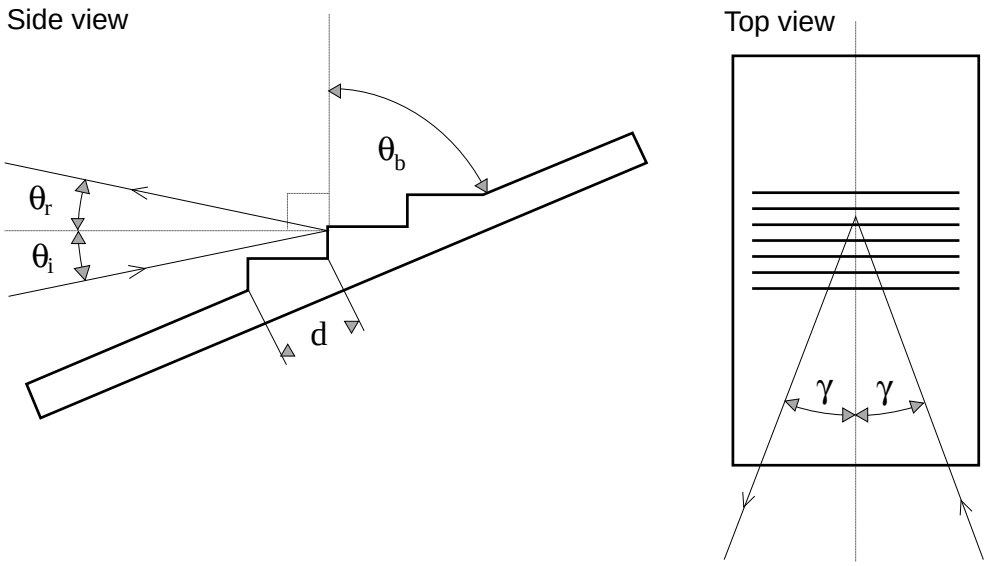

Figure 5.3: Echelle grating parameters.

5.3 Grating Matrix G

Following the definitions of Schroeder [1970] the diffraction equation for an echelle grating is:

$$m\lambda = d\left[\sin(\theta_b + \theta_i) + \sin(\theta_b - \theta_i)\right]\cos\gamma \tag{5.22}$$

where: m = order number for wavelength λ.

The meaning of the other parameters are illustrated in Figure 5.3.

Note that equation 5.22 is independent of position. Similarly the position of the ray is largely independent of the angles. These two aspects of the transfer function can therefore treated separately.

The relationship between the coordinate system used and the grating is illustrated in Figure 5.4. The apparent “reversal" of the x axis is due to the reflection at the grating surface.

Considering the x,y position of the output beam it is clear that:

$$y_{out} = y_{in} \tag{5.23}$$

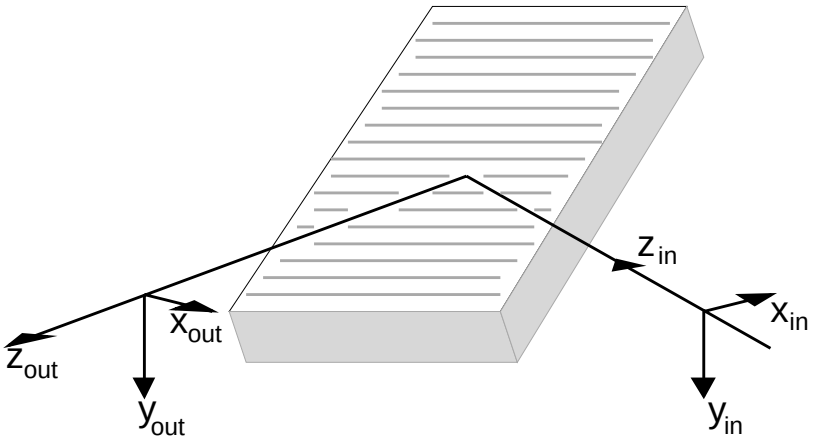

Figure 5.4: Analysis coordinates applied to the echelle grating.

and from the geometry of the grating, it can be shown that:

$$x_{out} = x_{in} + 2y_{in} \tan\theta_b \sin\gamma \tag{5.24}$$

Next the effect of the grating on the angular distribution of the beam is evaluated.

The angles from Figure 5.3 are related to the rays' altazimuth components by:

$$\begin{aligned} \phi_{y.in} &= -\Delta\theta_i \quad \phi_{y.out} = -\Delta\theta_r \\ \phi_{x.in} &= -\Delta\gamma \quad \phi_{x.out} = -\Delta\gamma \end{aligned} \tag{5.25}$$

As previously mentioned in Chapter 4, only the central wavelength of some order (any one will do) will be considered. Also the echelle is being used in a quasi-Littrow configuration, so for our principal ray:

$$\theta_i = \theta_r = 0 \tag{5.26}$$

giving

$$\frac{m\lambda}{d} = 2\sin\theta_b \cos\gamma \tag{5.27}$$

If we now consider an arbitrary input ray which differs from the principal ray by small angles, $\Delta\theta_i$,$\Delta\gamma$ then equation 5.22 can be rewritten to give:

$$\sin(\theta_b - \Delta\theta_r) = \frac{m\lambda}{d\cos(\gamma + \Delta\gamma)} - \sin(\theta_b + \Delta\theta_i) \tag{5.28}$$

Considering first order terns only, i.e. $(\Delta\gamma)^2 \approx 0$

$$\Delta\theta_r = \Delta\theta_i - 2\Delta\gamma \tan\gamma \tan\theta_b \tag{5.29}$$

Which from equation 5.25 can be written:

$$\phi_{y.out} = \phi_{y.in} - 2\phi_{x.in} \tan\gamma \tan\theta_b \tag{5.30}$$

Combining equations 5.23, 5.24, 5.25 and 5.30 the component matrix for the grating, G, is then:

$$G = \begin{vmatrix} 1 & 2\tan\theta_b \sin\gamma & 0 & 0 \\ 0 & 1 & 0 & 0 \\ 0 & 0 & 1 & 0 \\ 0 & 0 & -2\tan\theta_b \sin\gamma & 1 \end{vmatrix} \tag{5.31}$$

5.4 Grating Through-put

In this section the expected through-put (efficiency) of the echelle grating is calculated. The grating is 65°, 52.67 grooves / mm, used in quasi Littrow mode with γ = 10°.

Because the angular spread of each order is small, any wavelength will appear in some order near the blaze peak. There is, however an intensity distribution across the blaze peak which is determined by the effective width of a single echelle groove. This is given by:

$$I(\delta) = \left(\frac{\sin\delta}{\delta}\right)^2 \tag{5.32}$$

where δ is the phase difference between the centre and edge of a single groove of effective width D. Keeping the definitions from the previous section of this chapter, in quasi Littrow mode

$$D = d\cos\theta_b \tag{5.33}$$

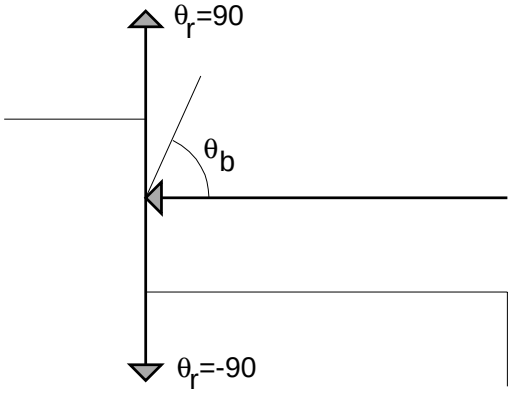

Figure 5.5: Angular range for diffracted light rays.

and

$$\delta = \frac{2\pi}{\lambda} D \frac{\sin\theta_r}{2} \tag{5.34}$$

To find the efficiency of an echelle grating it is necessary to calculate the distribution of light of a given wavelength across all orders for which $|\theta_r| < 90^\circ$ as shown in Figure 5.5.

The efficiency can then be calculated for each wavelength by

$$\varepsilon_\lambda = \frac{I_{m0}}{\sum_m I_m} \tag{5.35}$$

where I_{m0} = the relative intensity of light in the order being used
and I_m = the relative intensity of light in order m.

Clearly for positive values of θ_r there are no problems, however for $\theta_r < 0$ part (or all) of the light will undergo a second reflection from the top of the grooves as shown in Figure 5.6.

Once any secondary reflections are taken into account equation 5.35 can be used to calculate the theoretical efficiency over the whole spectrum. This is shown for parts of the spectrum in the Figure 5.7. Note also the variation in spectral coverage for the different orders.

These graphs are theoretical values and do not take into account reflectivity or irregularities in the groove surfaces. A scaling factor must

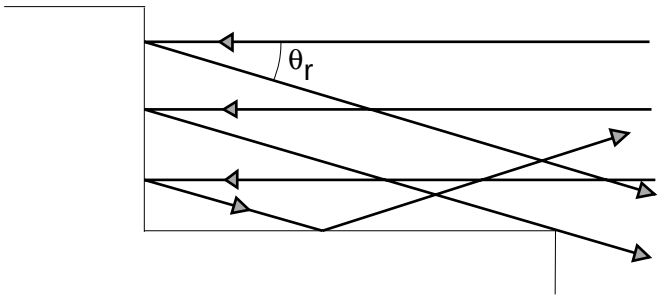

Figure 5.6: Diffracted light with partial secondary reflection.

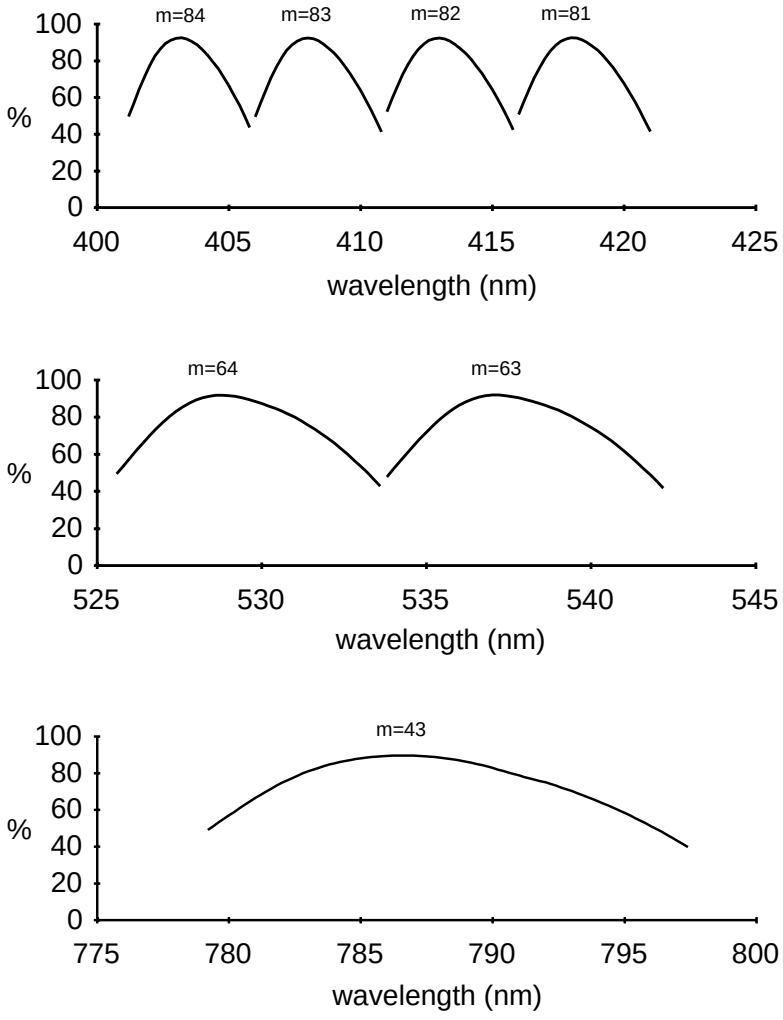

Figure 5.7: Theoretical echelle efficiencies.

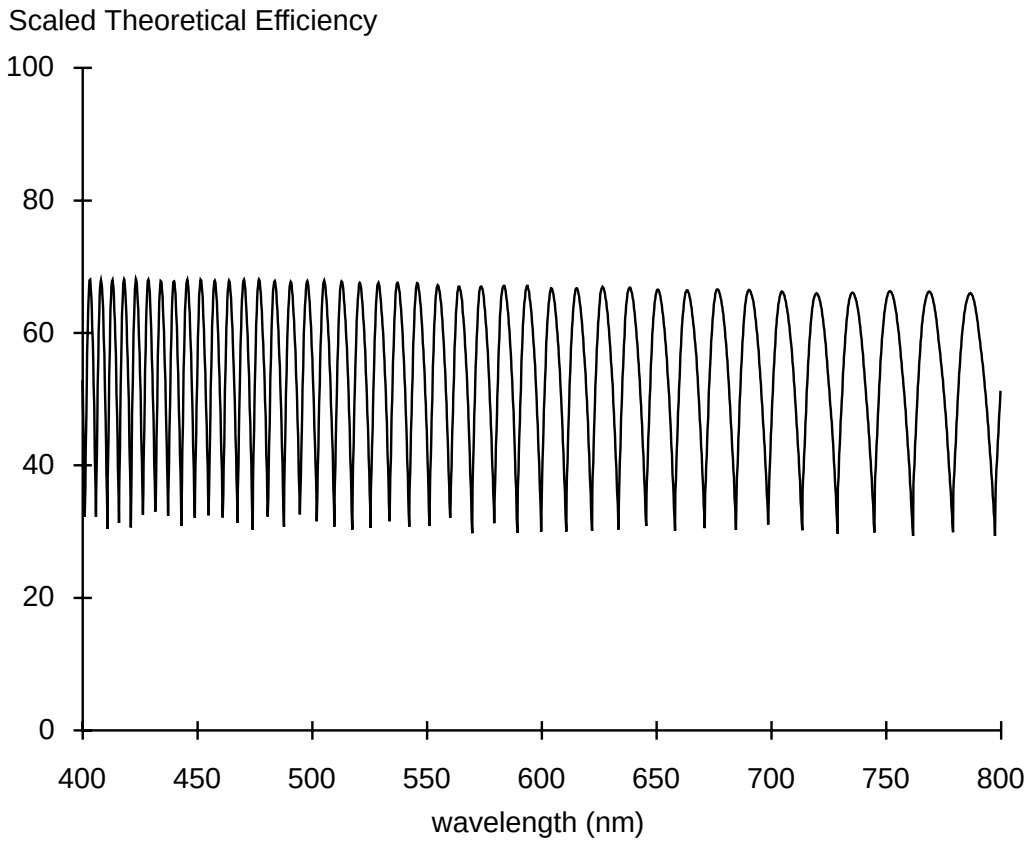

Figure 5.8: Theoretical echelle efficiencies scaled to match manufacturer's quoted values.

therefore be applied to the calculated efficiencies. Schroeder and Hilliard [1980] showed measured efficiencies of 60-65% for echelles in quasi-Littrow mode. A value of 67% at 546.1nm is quoted by the manufacturer of our grating (Milton Roy). Scaled results are shown in Figure 5.8.

Maximum through-put (efficiency) is clearly at the centre of the orders with a value of 67%. A minimum of 30% is found at the ends of the free spectral ranges. Both these values are substantially constant (within a few percent) over the range of spectral coverage. Therefore:

$$\begin{aligned} \tau_{grating.mboxmax} &\approx 0.67 \\ \tau_{grating.mboxmin} &\approx 0.30 \end{aligned} \tag{5.36}$$